Internal Motion of Lysozyme Studied by Time-Resolved Fluorescence Depolarization of Tryptophan Residues

Etsuko Nishimoto,[‡] Shoji Yamashita,*[,§] Arthur G. Szabo,[||] and Taiji Imoto[⊥]

Kyushu National Industrial Research Institute, Shuku-machi, Tosu, Saga 841, Japan, Institute of Biophysics, Faculty of Agriculture, Kyushu University, Higashi-ku, Fukuoka 812-81, Japan, Department of Chemistry and Biochemistry, University of Windsor, Ontario N9B3P4, Canada, and Faculty of Pharmaceutical Science, Kyushu University, Maidashi, Higashi-ku, Fukuoka 812-81, Japan

Received July 30, 1997; Revised Manuscript Received January 19, 1998

ABSTRACT: The internal motion of lysozyme was described by the steady-state and time-resolved fluorescence anisotropy of its tryptophan residues. The fluorescence of mutant lysozymes W62Y- and W108Y-lysozyme, in which Trp62 or Trp108 of hen egg white lysozyme was replaced with a tyrosine residue, could be respectively assigned to Trp108 or Trp62 at the longer wavelength region of the total fluorescence spectrum. The segmental motion of Trp62 as shown by its fluorescence anisotropy decay was described with two components originating from the fluctuational rotation of an indole moiety about the $C_\alpha-C_\beta$ bond and rotational wobble of the peptide segment adjacent to Trp62. Although Trp62 showed a high degree of motional freedom, its motion was significantly suppressed by the interaction of the mutant protein with a trimer of *N*-acetyl-D-glucosamine. By contrast, the segmental motion of Trp108 is hindered by the local cage structure at temperatures below 30 °C, but Relief from restricted motion occurred on the formation of ligand complex or by thermal agitation. Because of overlaps of the fluorescence spectrum, it is difficult to assign the segmental motion of Trp28 or Trp111, the other two tryptophan residues in lysozyme. However, a careful analysis of the fluorescence anisotropy decay of W62Y- and W108Y-lysozyme showed that the fluctuation of the hydrophobic matrix box was greater than that expected from lysozyme's crystal structure, although it was suppressed by the binding of the ligand to the active site of lysozyme.

Proteins are aperiodic long-chain polymers, and their tertiary structure is determined by weak noncovalent interactions between the amino acid subunits of the polypeptide. Structural fluctuation occurs intrinsically around an average atomic configuration. The molecular dynamics of proteins has become a matter of great interest among many biologists and biochemists. Most globular proteins undergo conformational alteration when they interact with small molecules and other proteins. Such conformational flexibility is an essential component of many biological systems. For example, in hormone−receptor binding, a conformational transition usually occurs for the transmission of signaling information, the ligand-induced conformational change being the main part of the cooperativity, while small fluctuational motions in some enzyme systems are required to complete the catalytic activity. Thus, to understand the full details of protein function also requires knowledge of the molecular dynamics of the internal protein motion.

Many physicochemical methods and techniques have been applied to study protein dynamics. X-ray crystallography provides the atomic position in a static structure of a protein. Temperature factors are thought to give some suggestion of protein structural flexibility. However, to determine the dynamics of the internal motion of a protein, other methods, such as nuclear magnetic resonance, infrared spectroscopy, or fluorescence depolarization studies, are used. These methods give parameters which describe the conformational fluctuation of a protein. The method used depends on the conditions of the systems being investigated. Fluorescence anisotropy is a unique method to measure the physical parameters of protein dynamics. The time-correlation function, which is generally used for the description of the dynamics, can be determined from such measurements. Fluorescence anisotropy studies using tryptophan or tyrosine residues as the fluorescence probe provide useful insight into the internal motions and conformational dynamics of proteins (*1, 2*). High sensitivity and picosecond time resolution are the bases for its use in studying protein dynamics. However, the use of time-resolved fluorescence anisotropy has been limited, because the method requires specific protein fluorophores in a protein for quantitative measurements. In the case of proteins containing a single tryptophan, the dynamics of the internal motion of the protein can be examined through the spectroscopic measurement of the tryptophyl fluorescence (*3*). X-ray crystal structures, when available, can be used to confirm the validity of the information obtained from the fluorescence anisotropy measurement. When proteins contain more than one tryptophan residue, ambiguities in the data rationalization are inevitable because of the spectral overlap of the tryptophyl fluorescence. The discrimination

* To whom correspondence should be addressed. Fax: +81-92-642-2879. E-mail: yamashita@agr.kyushu-u.ac.jp.
[‡] Kyushu National Industrial Research Institute.
[§] Faculty of Agriculture, Kyushu University.
[||] University of Windsor.
[⊥] Faculty of Pharmaceutical Science, Kyushu University.

S0006-2960(97)01865-5 CCC: $15.00
Published on Web 03/27/1998

of the fluorescence of the individual tryptophan residues in multi-Trp proteins has been a subject of considerable interest in itself. Mutant proteins can be produced where a selected tryptophan residue is replaced with other amino acids, permitting the investigation of the internal motions at different locations in the protein (*4*, *5*).

Hen egg white lysozyme (HEWL)[1] is one example of a multi-tryptophan protein, with tryptophan residues at locations 28, 62, 63, 108, 111, and 123. It offers the possibility of correlating its dynamics with enzymatic activity using the fluorescence spectroscopy of the individual tryptophan residues. Its high-resolution crystal structure shows that the two dominant fluorophores, Trp62 and Trp108, are arranged close to the substrate binding site. They play important roles in binding with a substrate or an inhibitor and in stabilizing the structure. Fluorescence analyses of these tryptophan residues have provided information on the lysozyme−ligand interaction and ligand-induced conformational change around the binding site (*6*). Because of the spectral overlap of the fluorescence among the four tryptophan residues in HEWL, there are some ambiguities in the interpretation of the data. Recently, we were able to resolve the unique fluorescence spectra of Trp62 and Trp108 using lysozyme mutants through fluorescence quenching techniques (*7*). The fluorescence maxima of Trp62 and Trp108 were found at 352 and 342 nm, respectively, while the fluorescence maxima of Trp28 and Trp111 occur at shorter wavelengths. These results were very useful in characterizing the ligand-induced conformational change in the different segments of the protein and in studies of segmental motions of each tryptophan residue. The molecular dynamics of the segmental motion of the tryptophans of HEWL has not been examined experimentally to date. Ichye and Karplus have reported their results using computer simulated fluorescence depolarization (*8*).

In this study the molecular dynamics of the internal motion in HEWL and the effect of ligand binding were investigated using the steady-state and time-resolved fluorescence anisotropy measurements of two lysozyme mutants, W62Y- and W108Y-lysozyme, where Trp62 or Trp108 was replaced with a tyrosine residue.

MATERIALS AND METHODS

Materials. HEWL recrystallized five times was purchased from Seikagaku Kogyo and was purified by cation-exchange chromatography. A (1→4)-linked trimer of *N*-acetyl-D-glucosamine [$(GlcNAc)_3$] was purchased from Sigma. CM-Toyopeal 650M, a cation-exchange resin, was obtained from Tosoh. A column of Wakosil 5C18-200 (4.6 × 250 mm) was obtained from Wako Pure Chemicals Institute. Chitin-coated Celite, which is an affinity absorbent for lysozyme, was prepared as described previously (*9*). Other chemicals were of analytical grade and were used without further purification.

Mutant Lysozymes. Two lysozyme mutants, W62Y-lysozyme and W108Y-lysozyme in which Trp62 and Trp108 were replaced with a tyrosine residue, respectively, were prepared following the method described previously (*10*). The mutants were expressed in *Saccharomyces cerevisiae* AH22 grown at 30 °C for 125 h. The mutant lysozymes secreted into the culture supernatant were isolated by cation-exchange chromatography (CM-Toyopeal 650M). The lysozyme was eluted by using a gradient of 0−0.5 M NaCl in sodium phosphate buffer (pH 7.0) and was collected, dialyzed against distilled water, and then lyophilized.

Steady-State Fluorescence Spectrum and Anisotropy. HEWL and mutant lysozymes were dissolved in sodium acetate buffer (pH 5.5, 100 mM). Steady-state fluorescence spectra were recorded on an SLM C-1000 fluorescence spectrophotometer. Each emission spectrum was strictly corrected for the excitation−detection response of the instrument and for stray light.

Steady-state fluorescence anisotropy (r_s) calculations were based on eq 1

$$r_s = (I_{||} - GI_{\perp})/(I_{||} + 2GI_{\perp}) \quad (1)$$

where $I_{||}$ and $I_{\perp}$ were the intensities of the parallel and perpendicular components, respectively, and G was the grating factor. The $I_{||}$ and $I_{\perp}$ values were detected simultaneously using the T-format configuration of the SLM C-1000. One Glan−Taylor polarizer was set vertically on the excitation side, and two other polarizers, one set in a vertical plane and the other in a horizontal plane, were located in the emission collection beam. The *G*-factor was obtained by measuring the intensity ratio of $I_{||}$ and $I_{\perp}$ with horizontally polarized excitation.

Fluorescence Decay Kinetics. The fluorescence decay measurements were performed using the laser/multichannel plate based time-correlated single photon counting technique. The excitation source was a sync-pumped argon ion dye laser. The excitation wavelength was 300 nm, and the emission was detected after passing through a monochromator with a 4-nm band-pass onto a microchannel plate photomultiplier tube. The channel width of the multichannel analyzer was 10 ps, and data were collected in 1024 channels. The instrumental response function was determined from the Raman scattering of D_2O. The laser/multichannel plate instrumentation used here was described elsewhere (*11*). Fluorescence decay data were analyzed by a nonlinear least squares iterative convolution method based on the Marquardt algorithm (*11*, *12*). Adequacy of the fitting was judged by inspection of the plots of weighted residuals and of statistical parameters such as sigma (σ) and the serial variance ratio (SVR) (*13*). For a satisfactory fit, the weighted residuals must be randomly distributed and σ and SVR should be in ranges of 1.0−1.2 and 1.8−2.0, respectively.

Fluorescence Anisotropy Decay. The fluorescence anisotropy decay measurement was performed by using the same instrument as the fluorescence decay measurement. But the parallel $I_{||}(t)$ and perpendicular $I_{\perp}(t)$ components were measured separately by orienting Glan−Taylor polarizers vertically and horizontally against the vertical excitation. $I_{||}(t)$ and $I_{\perp}(t)$ were deconvoluted and used to calculate $r(t)$ using equation 1. The *G*-factor in the wavelength region 300−400 nm was corrected by using azanaphthen in ethanol as an isotropic fluorescence standard. Adequacy of the fluorescence anisotropy decay was judged by the nonlinear

[1] Abbreviations: HEWL, hen egg white lysozyme; W62Y-lysozyme, hen egg white lysozyme in which Trp62 is replaced with tyrosine; W108Y-lysozyme, hen egg white lysozyme in which Trp108 is replaced with tyrosine; $(GlcNAc)_3$, (1→4)-linked trimer of *N*-acetyl-D-glucosamine; Trp, tryptophan; Tyr, tyrosine.

Table 1: Fluorescence Decay Parameters of Mutant Lysozymes and Complexes with $(GlcNAc)_3$[a]

	wavelength (nm)	τ_1 (ns)	τ_2 (ns)	τ_3 (ns)	τ_4 (ns)	α_1	α_2	α_3	α_4	σ	SVR
W62Y	320	2.90	1.17	0.42	0.05	0.06	0.31	0.37	0.26	1.02	2.00
	340	3.62	1.43	0.47	0.04	0.06	0.34	0.36	0.24	1.02	1.96
	380	3.86	1.51	0.56		0.15	0.54	0.31		1.01	1.98
W62Y-$(GlcNAc)_3$	320	1.77	0.71	0.05		0.17	0.63	0.20		1.05	2.00
	340	1.93	0.71	0.06		0.19	0.64	0.17		1.05	1.98
	380	2.28	0.71			0.29	0.71			1.00	1.90
W108Y	320	2.85	0.74	0.08		0.13	0.54	0.32		1.10	1.81
	340	3.61	1.57	0.55		0.19	0.36	0.45		1.00	2.00
	380	4.26	1.97	0.49		0.23	0.50	0.27		1.02	2.00
W108Y-$(GlcNAc)_3$	320	1.14	0.38			0.53	0.47			1.03	2.00
	340	1.51	0.43			0.46	0.54			1.01	1.96
	380	2.38	0.45			0.45	0.55			1.02	1.93

[a] Excitation wavelength, 300 nm.

least-squares curve fitting based on the Marquardt−Lebenberg algorithm (*14*).

Fluorescence Quenching by Acrylamide. The collisional quenching constant (k_q) of acrylamide against the fluorescence of mutant lysozymes was determined by using the well-known Stern−Volmer equation,

$$(I_0/I) - 1 = K_{SV}[Q] \quad (2)$$

where $K_{SV} = k_q\tau$; I_0 and I are the fluorescence intensities in the absence and in the presence of the quencher (Q), respectively; and τ and K_{SV} are the fluorescence lifetime and the Stern−Volmer constant, respectively. The fluorescence intensities at various wavelengths were measured by adding aliquots of a fleshly prepared solution of acrylamide with a constant concentration of the lysozymes. K_{SV} was obtained from the slope in Stern−Volmer plots, and k_q was calculated from K_{SV} and τ.

RESULTS

Fluorescence Spectrum. Figure 1 shows the fluorescence spectra of mutant lysozymes and their complexes with a trimer of *N*-acetyl-D-glucosamine [$(GlcNAc)_3$] in 0.1 M acetate buffer (pH 5.5). W108Y-lysozyme gave a fluorescence maximum at 342 nm similar to that of the fluorescence of HEWL. The fluorescence spectrum of W62Y-lysozyme, in which Trp108 was the most dominant fluorophore, occurs at the higher energy side, and its maximum wavelength was found at 336 nm. When W108Y-lysozyme formed a complex with $(GlcNAc)_3$, the fluorescence intensity was reduced about 10% and the fluorescence maximum shifted to 335 nm. On the other hand, W62Y-lysozyme showed an enhanced fluorescence and a shift to shorter wavelength evidenced by a shoulder near 320 nm in the complex with $(GlcNAc)_3$.

Fluorescence Decay Kinetics. The fluorescence decay kinetics of the mutant lysozymes and their complexes with $(GlcNAc)_3$ were measured across the entire fluorescence spectrum. The decay parameters at 320, 340, and 380 nm are listed in Table 1. The fluorescence decay kinetics of the free lysozyme showed three or four components depending on the fluorescence wavelength, with a greater number of components in the decay in the shorter wavelength region. One characteristic of the fluorescence decay of the mutants is that very short decay components, of the order of 40−80 ps, are seen at the shorter wavelength side but not at the longer wavelengths. The fluorescence decay kinetics of the

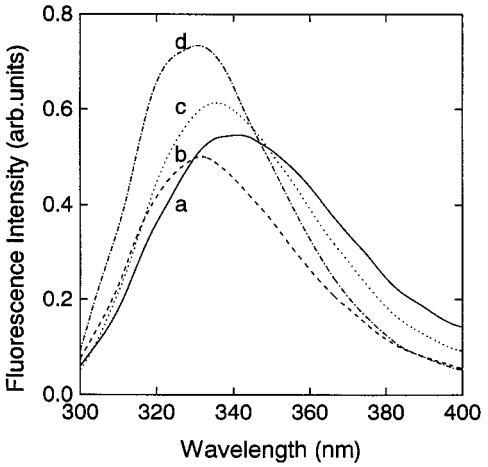

FIGURE 1: Fluorescence spectra of mutant lysozymes and their complex with $(GlcNAc)_3$. (a) W108Y-lysozyme. (b) W108Y-lysozyme-$(GlcNAc)_3$ complex. (c) W62Y-lysozyme. (d) W62Y-lysozyme-$(GlcNAc)_3$ complex. Concentrations of mutant lysozymes and $(GlcNAc)_3$ were 10 and 100 μM, respectively. Excitation wavelength, 300 nm. Temperature, 25 °C.

complex with $(GlcNAc)_3$ and the mutant lysozymes became simpler; that is, the number of components involved in fluorescence decay was reduced. The intensity weighted lifetime average was calculated by taking the mean of the intensity weighted lifetime, defined as $\tau_{av} = \Sigma\, \alpha_i\tau_i$, across the spectral region where measurements were taken. It was used to evaluate the collisional fluorescence quenching rate constant, k_q.

Collisional Fluorescence Quenching Constant. The Stern−Volmer constant (K_{SV}) of the fluorescence of mutant lysozymes was obtained from the slope in the plot of I_0/I against the concentration of acrylamide by using eq 2. The Stern−Volmer plots of the quenching of W108Y-lysozyme shown in Figure 2 was highly linear. The resulting K_{SV} depended on the emission wavelength. Similarly, the Stern−Volmer plot for W62Y-lysozyme gave a linear relationship between I_0/I and [Q] at several wavelengths. The collisional fluorescence quenching rate constants of W62Y-lysozyme, W108Y-lysozyme, and their complexes with$(GlcNAc)_3$ calculated from the mean intensity weighted lifetime and Stern−Volmer constants (K_{SV}) are given in Figure 3 together with the respective fluorescence spectra. The collisional quenching rate constants of the mutant lysozymes and their complexes with $(GlcNAc)_3$ were constant at wavelengths longer than their fluorescence maxima. Each tryptophan residue retains its individual collisional quenching rate

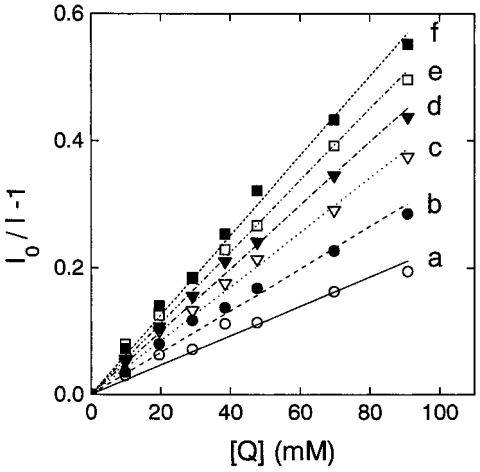

FIGURE 2: Emission wavelength dependence of Stern−Volmer plots for the fluorescence quenching of W108Y-lysozyme by acrylamide. Lines a, b, c, d, e, and f are plots for emission at 320, 330, 340, 350, 360, and 380 nm, respectively. The concentration of acrylamide is shown by [Q]. Plots are based on eq 2. Excitation wavelength, 300 nm. Temperature, 25 °C.

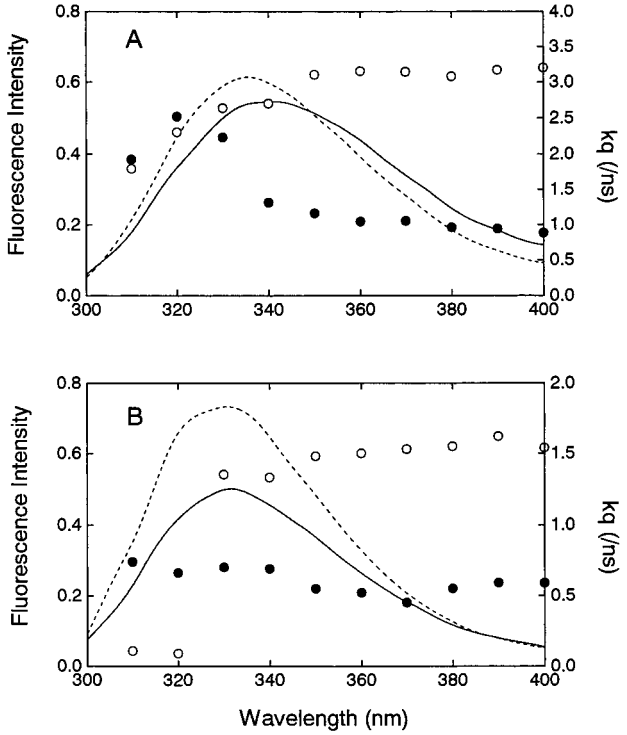

FIGURE 3: Emission wavelength dependence of the collisional fluorescence quenching constant (k_q) of free mutant lysozymes (A) and their complex with $(GlcNAc)_3$ (B). ○, W108Y-lysozyme; ●, W62Y-lysozyme. Solid and broken lines in panels A and B are fluorescence spectra of W108Y- and W62Y-lysozyme. The value of k_q was calculated from the average lifetimes and the Stern−Volmer constant (K_{SV}) using $k_q = K_{SV}/\tau$.

constant in accordance with its location in the protein. The values for each tryptophan must be constant regardless of the emission wavelength. Therefore, the independence of emission wavelength of k_q suggests that the fluorescence of W62Y- and W108Y-lysozymes and their complexes originates from Trp108 or Trp62, respectively, at wavelengths longer than 360 nm. Because Trp108 and Trp62 are in a polar environment, it is expected that their fluorescence should dominate at the lower energy side of the spectrum.

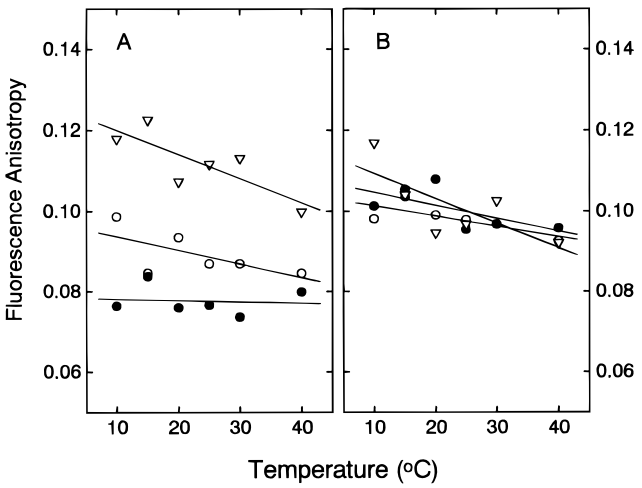

FIGURE 4: Steady-state fluorescence anisotropy of HEWL, W108Y-lysozyme, and W62Y-lysozyme (A) and their complexes with $(GlcNAc)_3$ (B). ○, HEWL; ●, W108Y-lysozyme; ▽, W62Y-lysozyme. Concentration of the lysozymes, 10 μM; concentration of $(GlcNAc)_3$, 1 mM; excitation wavelength, 300 nm; emission wavelength, 380 nm.

Steady-State and Time-Resolved Fluorescence Anisotropy. Figure 4 shows the steady-state fluorescence anisotropy of HEWL and of W62Y- and W108Y-lysozyme (Figure 4, panel A) and their complexes with $(GlcNAc)_3$ (Figure 4, panel B). When the steady-state fluorescence anisotropy was measured at 380 nm with excitation at 300 nm, W62Y-lysozyme gave larger values than W108Y-lysozyme. Since their molecular weights are identical, this difference in the fluorescence anisotropy value can be rationalized as being due to differences in the internal motion of the respective tryptophan residues. The fluorescence of W62Y-lysozyme and W108Y-lysozyme at 380 nm is attributed to Trp108 and Trp62, respectively. Therefore, it is concluded that Trp62 has a higher degree of fluctuation than Trp108. The fluorescence anisotropy of HEWL showed an intermediate value between those of the W62Y and W108Y mutants. The fluorescence of HEWL consists of contributions from both Trp62 and Trp108 at 380 nm. In the complex of W108Y-lysozyme with $(GlcNAc)_3$, the fluorescence anisotropy of W108Y-lysozyme increased by 25%, indicating that the internal motion of Trp62 in the complex was restricted. Although the fluorescence anisotropy of HEWL also increased in the complex, it is noteworthy that W62Y-lysozyme had a lower anisotropy in the complex with the ligand than did the mutant in the absence of substrate. This suggests that the internal motion of Trp108 becomes less restricted in the complex, in contrast to the case of Trp62.

The fluorescence anisotropy decay profiles of the two mutant lysozymes, W108Y- and W62Y-lysozyme, monitored at 380 nm are shown in Figure 5. The fluorescence anisotropy of W108Y-lysozyme decayed faster than that of W62Y-lysozyme. The fluorescence anisotropy decay of the W108Y-lysozyme−ligand complex (Figure 6) shows a slower decay than that of the free mutant lysozyme. These results support the suggestion obtained from the steady-state anisotropy studies that Trp62 fluctuates more freely than Trp108 in the free enzyme and that the internal motion of Trp62 becomes restricted in the interaction with $(GlcNAc)_3$. The ligand-induced change in the fluorescence anisotropy

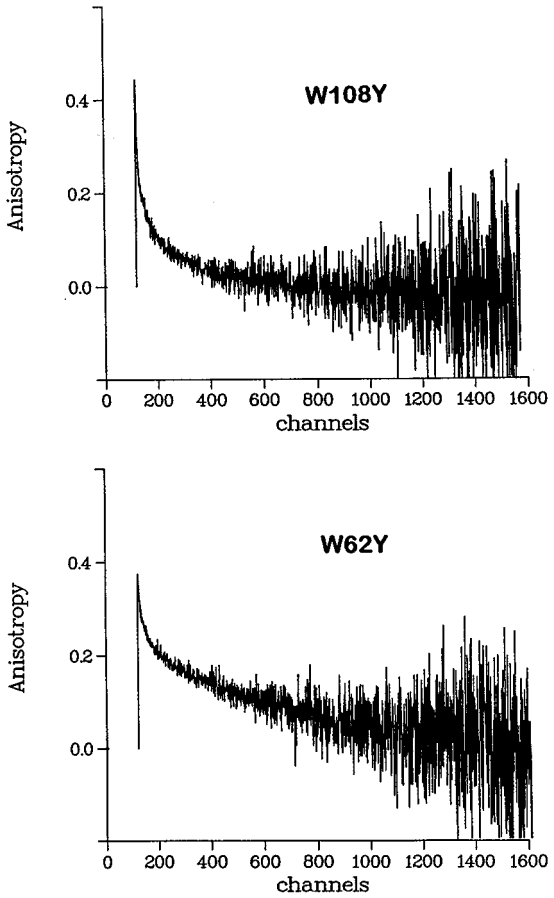

FIGURE 5: Fluorescence anisotropy decay of W108Y- (top) and W62Y-lysozyme (bottom). Excitation wavelength, 300 nm; emission wavelength, 380 nm; bandwidth, 4 nm; channel width, 10 ps. Concentration of the mutant lysozymes was 10 μM. Temperature, 25 °C.

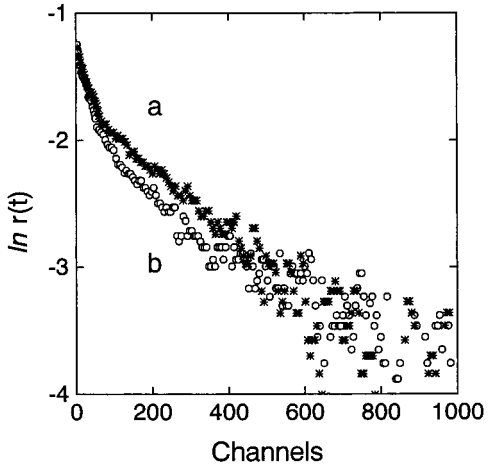

FIGURE 6: Semilog plot of the fluorescence anisotropy decay of W108Y-lysozyme (b) and the complex with $(GlcNAc)_3$ (a). The excitation and emission wavelengths were 300 and 380 nm, respectively. Channel width 10 ps. Concentration of W108Y-lysozyme, 10 μM. The anisotropy decay of the complex was observed in the presence of 1 mM $(GlcNAc)_3$. Temperature, 25 °C.

decay of W62Y-lysozyme could not be clearly recognized by a visual inspection of the decay profile. By contrast, the fluorescence anisotropy of Trp108 in W62Y-lysozyme decayed faster in the complex with $(GlcNAc)_3$. Analysis of the fluorescence anisotropy decay in terms of a linear combination of exponentials, as in eq 3,

$$r(t) = \Sigma \beta_i \exp(-t/\phi_i) \tag{3}$$

where ϕ_i is the rotational correlation time of the i-th component and β_i is the corresponding amplitude, characterized the segmental motions of Trp62 and Trp108 and their responses to ligand binding. The resulting decay parameters are summarized in Table 2. Each fluorescence anisotropy decay showed one rotational correlation time between 4 and 4.6 ns. This value is consistent with the rotational correlation time for the whole-body rotation of lysozyme calculated by the Einstein−Stokes relationship, $\phi = \eta V/kT$, where η is the viscosity of water, V is the hydrated volume of lysozyme, k is the Boltzman constant, and T is the absolute temperature. The anisotropy decay of W108Y-lysozyme was best fit to triple-exponential decay kinetics characterized by correlation times of $\phi_1 = 0.05$ ns, $\phi_2 = 0.53$ ns, and $\phi_3 = 4.12$ ns. The shorter correlation times are assigned to the local segmental motion of Trp62. The fractional amplitudes,

$$f_1 = \beta_1/\Sigma \beta_i, \qquad f_2 = \beta_2/\Sigma \beta_i \tag{4}$$

which are a measure of the freedom of the segmental motion, were 0.11 and 0.46, respectively. The fluorescence anisotropy decay of Trp108 in W62Y-lysozyme was described by a double-exponential function and one of the two correlation times corresponding to the whole-body rotation of the lysozyme. The fractional amplitude of the fast decay component was small and was estimated to be 0.22.

Table 2: Anisotropy Decay Parameters of Mutant Lysozymes and Complexes with $(GlcNAc)_3$[a]

	β_1	β_2	β_3	ϕ_1 (ns)	ϕ_2 (ns)	ϕ_3 (ns)	f_1 (%)	f_2 (%)	f (%)
W108Y	0.03	0.13	0.12	0.05	0.53	4.12	11	46	57
W108Y-$(GlcNAc)_3$	0.10		0.20	0.26		4.00	33		33
W62Y	0.06		0.21	0.22		4.60	22		22
W62Y-$(GlcNAc)_3$	0.07		0.22	0.22		4.50	24		24

[a] Excitation wavelength, 300 nm; emission wavelength, 380 nm; temperature, 30 °C.

The fluorescence anisotropy decay of W108Y-lysozyme was drastically changed by the interaction with $(GlcNAc)_3$ as seen in Figure 6. The decay kinetics became a double-exponential function with the correlation times 0.26 and 4.0 ns. The segmental motion of Trp62 was suppressed by the binding of $(GlcNAc)_3$ as shown by the reduction of the fractional amplitude of the fast decay component previously assigned to the segmental motion. In the case of W62Y-lysozyme, the amplitude of the fast decay component of W62Y-lysozyme increased in the complex with $(GlcNAc)_3$. This result was consistent with the ligand binding effect of the increased steady-state fluorescence anisotropy of this mutant. To obtain more detailed information on the dynamics of the internal motion of lysozyme, the temperature dependence of the anisotropy decay behavior was investigated at various temperatures. Figure 7 shows the temperature dependence of the normalized amplitude [$f = \beta_1/(\beta_1 + \beta_2)$] and the rotational correlation time of the faster decay component of W62Y-lysozyme. The fractional amplitude decreased with increasing temperature from 10 to 30 °C, while the fast rotational correlation time appeared to be

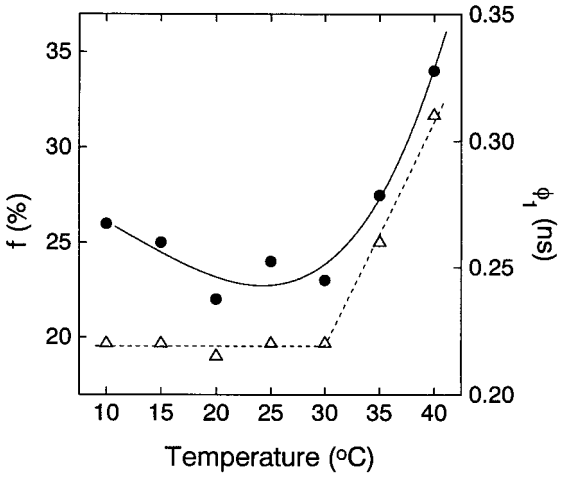

FIGURE 7: Temperature dependence of the motional freedom and corresponding rotational correlation time of Trp108 in W62Y-lysozyme. ●, motional freedom (*f*); △, rotational correlation time (ϕ_1). Values for *f* and ϕ_1 are given in eqs 3 and 4.

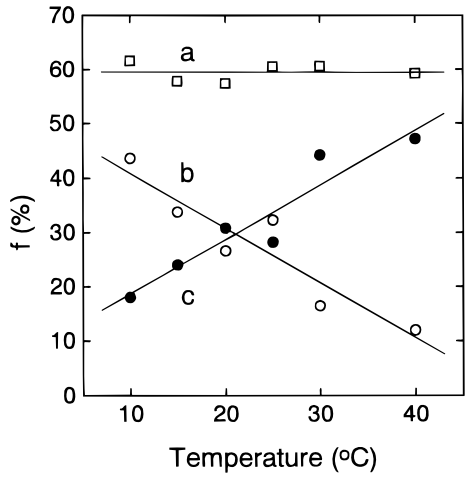

FIGURE 8: Temperature dependence of the rotational freedom of Trp62 in W108Y-lysozyme. Plot a, total freedom; plots b and c, the freedom of the rapid and moderate decay components, respectively.

insensitive to a variation of temperature over this range. As shown in Figure 7, the fractional amplitude and the correlation time of the segmental motion abruptly increased at temperatures higher than 30 °C.

The temperature dependence of the segmental motion of Trp62 in W108Y-lysozyme as determined from fluorescence anisotropy decay measurements is shown in Figure 8. The sum of the fractional amplitudes of the two segmental motions remained constant at 0.6 and almost independent of temperature in the range 10−40 °C. However, the fractional amplitude of the faster motion decreased, in contrast with that of the slower motion, whose fractional amplitude increased with increasing temperature. The temperature dependence of the rotational correlation times of W108Y-lysozyme was investigated to evaluate the activation energy for the segmental motion of the Trp62 residue. The faster and slower components gave a linear relationship in Arrhenius plots, shown in Figure 9. The activation energies estimated from the slopes were 0.8 eV (18.3 kcal/mol) and 0.35 eV (8.0 kcal/mol) for the faster and the slower segmental motions, respectively.

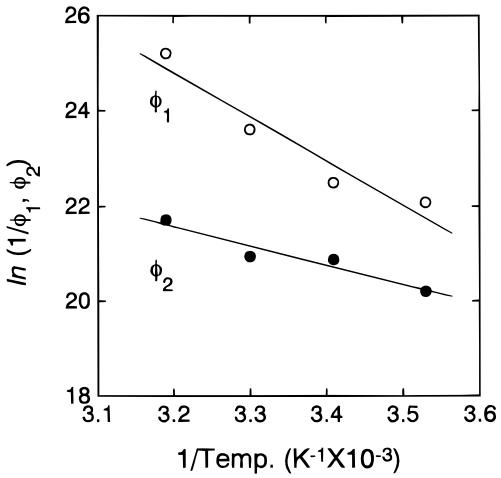

FIGURE 9: Arrhenius plot for the reciprocals of the rotational correlation times of Trp62 in W108Y-lysozyme. The symbols ϕ_1 and ϕ_2 represent the rotational correlation times of the faster and slower relaxing components in the fluorescence anisotropy decay.

The fluorescence anisotropy decay kinetics of W62Y- and W108Y-lysozyme measured at 320 nm were described by double and triple exponentials, respectively. The rotational correlation time of the slowest decay component was consistent with that expected for the whole-body rotation of lysozyme. The faster anisotropy decay times of these mutants were 0.18 ns for W62Y-lysozyme and 0.05 and 0.51 ns for W108Y-lysozyme at this emission wavelength. Also at 320 nm, the fluorescence anisotropy decay kinetics of W108Y-lysozyme changed to a double-exponential function in the interaction with $(GlcNAc)_3$, resulting in the reduction of the motional freedom of the tryptophan residue.

DISCUSSION

The independence of the collisional fluorescence quenching rate constants of W62Y- and W108Y-lysozyme at fluorescence wavelengths greater than 360 nm suggests that the fluorescence of mutant lysozyme originated from a single tryptophan residue. It has been well established that Trp63 and Trp123 do not contribute significantly to the fluorescence of lysozyme (*15*). This allows one to assign the fluorescence to Trp62 or Trp108 in the low energy spectral range and to characterize the dynamics of the segmental motion of Trp62 or Trp108 by measuring the fluorescence anisotropy at wavelengths longer than 360 nm.

The fluorescence anisotropy decay kinetics, $r(t)$, are related to the steady-state anisotropy, r_s by eq 5,

$$r_s = \int F(t) \cdot r(t)\, dt \,/\, \int F(t)\, dt \qquad (5)$$

where $F(t)$ is the total fluorescence intensity decay. The parameters obtained for the anisotropy decay of W108Y- and W62Y-lysozyme were fully consistent with the steady-state anisotropy. The initial anisotropy ($t = 0$), which is given by $r_0 = \Sigma\beta_i$, is decided by the absorption and fluorescence transition moment directions and contributes to the depolarization processes of tryptophan residues in proteins. Parvalbumin and M13 coat protein of bacteriophage give the largest (0.34) and the smallest (0.14) values, respectively, for r_0 of a single tryptophan residue in a protein (*16, 17*). In the experiments reported herein the excitation was at 300 nm to avoid excitation of tyrosine residues, and the observed

r_0 values for the mutant lysozymes were within a reasonable range (0.27−0.30). This suggests that the fluorescence anisotropy measurements do not include any substantial artifacts.

The anisotropy decay of W108Y-lysozyme monitored at 380 nm, which originates from fluorescence of Trp62, was described by a triple-exponential decay function. Since the longest rotational correlation time is consistent with that expected for the whole-body rotation of the mutant lysozyme, the other two components can be assigned to the local segmental motion of Trp62. The correlation times of these two segmental motions were in the time ranges 20−200 and 0.3−2.1 ns, respectively, depending on the temperature. It is possible that rotation of the indole moiety around the $C_\alpha-C_\beta$ bond or wobbling of the hinge site to which Trp62 is attached may be responsible for the rotational fluctuation of Trp62 (*18*). The time scales of the two rotational correlation times suggest that the faster component may correspond to the indole rotation around $C_\alpha-C_\beta$ and the slower to the wobbling of the hinge position. The activation energy for this segmental motion suggests that wobbling of the peptide main chain which results in the medium correlation time is sensitive to thermal activation. As the temperature increased, this motion became more pronounced. On the other hand, apparently the motional freedom of the rotation of $C_\alpha-C_\beta$ deceased with increasing temperature. This inverse correlation between these two segmental motions is interesting to consider in terms of the internal motion of the whole protein.

The segmental motion of Trp108 as revealed by the fluorescence anisotropy decay of W62Y-lysozyme at 380 nm was described by a single fast component of the exponential anisotropy decay function at 10−30 °C. The correlation time of Trp108 corresponds to the faster of the two segmental motions of Trp62, and it is therefore assigned to the rotation of the indole moiety around the $C_\alpha-C_\beta$ bond. Trp108 is surrounded by polar amino acids in a cage structure of the peptide backbone according to the crystal structure and the Raman spectra of HEWL (*19*−*21*). It is anticipated that the segmental motion of Trp108 would be restricted. Indeed, its motional freedom was low and within the range 0.27−0.20. As the temperature increased to >35 °C, the rotational correlation time and the motional freedom increased abruptly. Considering the similarity in the response of the motional freedom to temperature, it is interesting to speculate that the segmental motion of Trp108 changed from being due to the rotation around the $C_\alpha-C_\beta$ bond to the wobbling of the hinge point where Trp108 is attached at this temperature. Probably, two types of internal motion may be allowed for Trp108 at the higher temperature. It was not possible to separate the parameters which describe these motions for Trp108.

Because of the fluorescence spectral overlap of Trp28 and Trp111 with Trp62 or Trp108, it is not possible to definitely describe the segmental motion of either Trp28 or Trp111. It is possible, however, to discuss their motion in terms of the segmental motion of Trp62 or Trp108 as determined above from measurements at wavelengths greater than 360 nm. The fluorescence anisotropy decay of W62Y-lysozyme monitored at 320 nm was described by a double-exponential function. It showed a higher order parameter than the measurements at 380 nm. According to Nishimoto and coworkers, the fluorescence which Trp108 contributed to the total fluorescence at 320 nm was 50% (*7*). If one assumes that the measured anisotropy decay parameters were averaged according to their fluorescence contribution to the total fluorescence, then the motional freedom of Trp28 or Trp111 is estimated to be 0.38 in the W62Y-lysozyme. Similarly, the motional freedom of Trp28 or Trp111 of W108Y-lysozyme was smaller and was estimated to be 0.17. These approximations imply that the segmental motion in the hydrophobic matrix box is much greater than that predicted from the X-ray structure of HEWL. It is also interesting to note that the segmental motion in the hydrophobic matrix was lowered by the replacement of Trp108 with a tyrosine residue, the latter having a smaller molecular size than a tryptophan residue. Ichye and Karplus had applied molecular dynamics simulations to the fluorescence depolarization of the individual tryptophan residues in HEWL. They showed that Trp62 retained extensive motional freedom but that the segmental motions of Trp28 and Trp111 were suppressed (*8*). Their simulations seem not to be fully consistent with our results. But the discrepancy recognized for the motion at the hydrophobic matrix box region is caused by the short time interval on the simulation. It is shown that positional rms fluctuations of main chain and side chain atoms become larger as the time-averaging period increases in recent molecular dynamic studies (*22*−*24*). Cross and Fleming showed that the fluctuational motion was active at the hydrophobic matrix box region using the fluorescence depolarization of eosin bound to tyrosine (*25*). Their report is also consistent with the results reported in this work.

Recently, we reported that HEWL subtly alters its conformation depending on the interaction with a ligand such as $(GlcNAc)_3$ (*7, 26*). The effects of ligand binding on the steady-state and time-resolved fluorescence anisotropy of mutant lysozymes demonstrate that the segmental dynamics of the tryptophan residues change at the same time as the conformational changes that are related to ligand binding. The increase in the steady-state anisotropy and the lengthening of the anisotropy decay of W108Y-lysozyme at 380 nm revealed that the segmental motion of Trp62 is restricted in the lysozyme complex with $(GlcNAc)_3$. The fluorescence anisotropy decay kinetics of the W108Y-lysozyme−$(GlcNAc)_3$ complex was changed and was described by a double-exponential decay, indicating that the segmental motion was reduced to a single type. Although it is not possible to decide which component, the faster or the slower, changed, the motion was restricted by the interaction. We propose from earlier published evidence that the wobbling motion of Trp62 was suppressed. In experiments where Trp62 in HEWL was chemically modified to kynurenine (*27*), the fluorescence anisotropy decay monitored at 450 nm with 360-nm excitation showed that the segmental motion of Kyn62 in Kyn62-lysozyme could be described by double-exponential kinetics, one being rapid and the other slower, similar to that observed for Trp62 in W108Y-lysozyme. When $(GlcNAc)_3$ was bound to Kyn62-lysozyme, only the slower segmental motion of kynurenine was completely inhibited. The fluctuation of Trp108 was considerably limited in the peptide cage in the free enzyme. The freedom of the segmental motion increased when W62Y-lysozyme interacted with $(GlcNAc)_3$. This result is also supported by the steady-state fluorescence anisotropy of W62Y-lysozyme, suggesting that the segmental motion of Trp108 becomes liberated from motional restriction in this peptide cage when $(GlcNAc)_3$ binds to this protein.

The degrees of freedom of the segmental motion of Trp28/Trp111 and Trp62 or Trp108 in the mutant lysozymes, allocated according to their fluorescence contribution at 320 nm, were reduced to 0.36 and 0.05 in W62Y- and W108Y-lysozyme on formation of the complex with the substrate. This suggests that the binding effect of $(GlcNAc)_3$ extends to the hydrophobic matrix box region and restricted the segmental motions of Trp28/Trp111. Because of the overlapping fluorescence of Trp62 or Trp108 and Trp28/Trp111, the results of fluorescence quenching experiments inevitably include some ambiguity. However, the reduction of the collisional quenching rate constant for the fluorescence of Trp28/Trp111 in the lysozyme−$(GlcNAc)_3$ complex is consistent with the results in the fluorescence depolarization studies.

Neither Trp108 nor Trp28/Trp111 takes part directly in the binding with $(GlcNAc)_3$. Nevertheless, the conformations and dynamic properties of these tryptophan residues are modified in the formation of the complex. Nishimoto and coworkers showed a spectral change in the quenching resolved fluorescence spectra of Trp28/Trp111 due to the Trp108-dependent conformational deformation (*7*). Lumb and coworkers suggested that the ligand-induced conformational change around Trp28 was closely related to that of Trp108 from analysis of the chemical shift in ^1H nuclear magnetic resonance studies (*28*). Although their work implied that the conformations of Trp108 and Trp28/Trp111 are mutually dependent on one another, the increase in the motional freedom of Trp108 may be caused by the restriction of the fluctuational motion at the hydrophobic matrix box. Trp28/Trp111 and Trp108, which are respectively arranged in the hydrophobic matrix and located adjacent to the binding site, construct a framework to maintain the structure of lysozyme. The changes in the dynamic properties of these tryptophan residues and the conformation of the lysozyme induced by the interaction with the ligand are very interesting considering the relationship between protein flexibility and structural stability.

The motional freedom, f_i, connected with the order parameter, S^2, gives information on the angular displacement, θ, responsible for the segmental motion of the tryptophan residue according to eq 6 (*29*):

$$S^2 = 1 - \Sigma f_i = {}^1/_2 \times \cos\theta\,(\cos\theta + 1) \qquad (6)$$

Figure 10 shows the effect of $(GlcNAc)_3$ binding on the angular displacement of the internal motion of Trp62, Trp108, and Trp28/Trp111. The angular displacement for the internal motion of Trp62 reduced from $\theta = 56°$ to $\theta = 42°$ on binding of $(GlcNAc)_3$. Then, the orientation of Trp62 with respect to Trp108 may change in the complex. It has been shown in the energy transfer experiment using Kyn62-lysozyme that kynurenine (Trp62) changed its orientation in such a way that the energy transfer efficiency from Trp108 to Kyn62 was enhanced (*30*). Trp108 is surrounded with polar side chains in the polypeptide cage and fluctuates more in the lysozyme−ligand complex. It is difficult to draw a definite picture for the segmental motions of Trp28 or Trp111 because the spectral separation of these residues is not yet possible. However, this work suggests that the segmental fluctuation of Trp28/Trp111 was suppressed in the hydrophobic matrix box region on the interaction of the mutant lysozyme with $(GlcNAc)_3$.

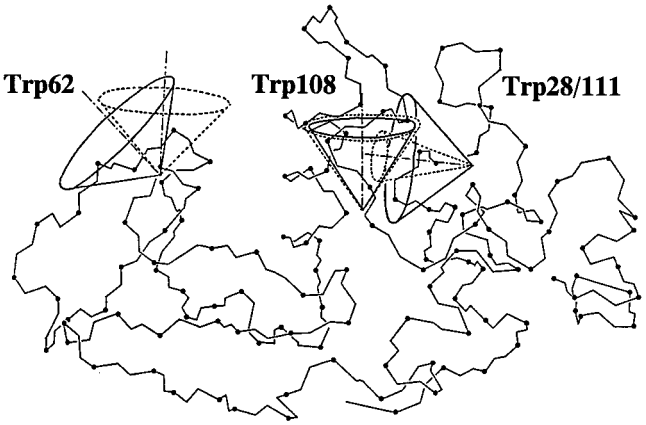

FIGURE 10: Changes in the segmental motion of Trp62, Trp108, and Trp28 on the formation of the $(GlcNAc)_3$ complex. Solid and broken line are the segmental motions of tryptophan residues unbound and bound lysozyme, respectively. Corn angle θ is estimated from order parameter $S^2 = \beta^p/\Sigma\beta_i = \cos\theta(\cos\theta + 1)$. Trp62 is represented in a parallel orientation to Trp108 in the unbound lysozyme. The motional freedom of Trp28/Trp111 is represented by the result in W108Y-lysozyme.

The fluorescence decay kinetics of the mutant lysozyme were also influenced by the binding of $(GlcNAc)_3$. This suggests that the dynamics of the internal motions of tryptophan residues in proteins correlate with the fluorescence decay properties of tryptophan residues. Harris and Hudson investigated the photophysical properties of tryptophan residues located in various environments using a single tryptophan containing T4 pharge mutant lysozyme (*4*). They concluded in their work that a conformationally heterogeneous state of amino acids proximate to a tryptophan residue was responsible for the fluorescence decay of the immobilized tryptophan residue in protein. The reduction of the number of the fluorescence decay components by the formation of the complex may be rationalized as the change in the conformational state around the tryptophan residue. Probably, the heterogeneity of the conformational state should be reduced by the restriction of the tryptophan's segmental motion in the mutant lysozyme.

In conclusion, we have shown that the segmental motions of four fluorescent tryptophan residues arranged around the binding site and in the hydrophobic matrix box region exhibit specific dynamic properties depending on their location and individual responses to interactions with ligand. Trp62, which is considered to be closely associated with the binding of the ligand, preserves a large degree of motional freedom, while on the other hand, the internal motion of Trp108 was restricted considerably in the vicinity of the binding site of HEWL. Although it has been considered that the hydrophobic matrix box of HEWL has a densely packed structure, the local segmental motions of Trp28/Trp111 appear to be greater than one might expect from the X-ray structure of the enzyme. On the binding with $(GlcNAc)_3$, the segmental motions of Trp62 and Trp28/Trp111 were suppressed while that of Trp108 was increased.

REFERENCES

1. Munro, I., Pecht, I., and Stryer, L. (1979) *Proc. Natl. Acad. Sci. U.S.A. 76*, 55−60.
2. Ferreira, S. T., Stella, L., and Gratton, E. (1994) *Biophys. J. 66*, 1185−1196.

3. Sopkova, J., Gallay, J., Vincent, M., Pancoska, P., and Lewit-Bentley, A. (1994) *Biochemistry 33*, 4490−4499.
4. Harris, D. L., and Hudson, B. S. (1990) *Biochemistry 29*, 6276−6285.
5. Vos, R., Engelborghs, Y., Izard, J., and Baty, D. (1995) *Biochemistry 34*, 1734−1743.
6. Lehrer, S. S. (1971) *Biochemistry 10*, 3254−3263.
7. Nishimoto, E., Yamashita, S., and Yamasaki, N. (1995) *Proceeding of 46th Symposium on Protein Structure (Japan)* (Suzuki, K., Ed.) pp 77−80, Protein Structure Society of Japan, Tokyo, Japan.
8. Ichye, T., and Karplus, M. (1983) *Biochemistry 22*, 2884−2893.
9. Yamada, H., Ito, Y., Fukumura, T., and Imoto, T. (1985) *Anal. Biochem. 146*, 71−74.
10. Inoue, M., Yamada, H., Yasukouchi, T., Kuroki, R., Miki, T., Horiuchi, T., and Imoto, T. (1992) *Biochemistry 31*, 5545−5553.
11. Willis, K. J., and Szabo, A. G. (1989) *Biochemistry 28*, 4902−4908.
12. Zuker, M., Szabo, A. G., Bramall, L., and Krajcarski, D. T. (1985) *Rev. Sci. Instrum. 56*, 14−22.
13. Darbin, J., and Watson, G. S. (1971) *Biometrika 58*, 1−19.
14. McKinnon, A. E., Szabo, A. G., and Miller, D. R. (1977) *J. Phys. Chem. 81*, 1564−1570.
15. Cowgill, R. W. (1967) *Biochim. Biophys. Acta 140*, 37−44.
16. Ferreira, S. T. (1989) *Biochemistry 28*, 10066−10072.
17. Datema, K. P., Visser, A. J. W. G., van Hoek, A., Wolfs, C. J. A. M., Spruijt, R. B., and Hemminga, M. A. (1987) *Biochemistry 26*, 6145−6152.
18. Gottlieb, Y., and Wahl, P. (1963) *J. Chem. Phys. 60*, 849−854.
19. Sternberg, M. J. E., Grace, D. E. P., and Phillips, D. C. (1979) *J. Mol. Biol. 130*, 231−253.
20. Blake, C. C. F., Johnson, L. N., Mair, G. A., North, A. C. T., Phillips, D. C., and Sarma, V. R. (1967) *Proc. R. Soc. London B167*, 378−388.
21. Miura, T., Takeuchi, H., and Harada, I. (1988) *Biochemistry 27*, 88−94.
22. Hünenberger, P. H., Mark, A. E., and van Gunsteren, W. F. (1995) *J. Mol. Biol. 252*, 492−503.
23. Smith, L. J., Mark, A. E., Dobson, C. M., and van Gunsteren, W. F. (1995) *Biochemistry 34*, 10918−10931.
24. Karplus, M., and Post, C. B. (1996) *EXS 75*, 111−141.
25. Cross, A. J., and Fleming, G. S. (1986) *Biophys. J. 50*, 507−512.
26. Yamashita, S., Nishimoto, E., and Yamasaki, N. (1995a) *Biosci. Biotechnol. Biochem. 59*, 1255−1261.
27. Yamashita, S., Nishimoto, E., and Yamasaki, N. (1995b) *Biosci. Biotechnol. Biochem. 59*, 1579−1580.
28. Lumb, K. J., Cheetham, J. C., and Dobson, C. M. (1994) *J. Mol. Biol. 235*, 1072−1087.
29. Lipari, G., and Szabo, A. (1982) *J. Am. Chem. Soc. 104*, 4559−4570.
30. Yamashita, S., Nishimoto, E., Szabo, A. G., and Yamasaki, N. (1996) *Biochemistry 35*, 531−537.

BI9718651